

Continuous 25-yr aerosol records at coastal Antarctica

Part 2: variability of the radionuclides ^7Be , ^{10}Be and ^{210}Pb

By CHRISTOPH ELSÄSSER^{1*}, DIETMAR WAGENBACH¹, ROLF WELLER²,
MATTHIAS AUER^{1,3,†}, ANTON WALLNER³ and MARCUS CHRISTL⁴, ¹*Institut für Umweltphysik,
University of Heidelberg, Im Neuenheimer Feld 229, D-69120 Heidelberg, Germany;* ²*Alfred Wegener Institute for
Polar and Marine Research, D-27570 Bremerhaven, Germany;* ³*Vienna Environmental Research Accelerator,
University of Vienna, A-1090 Vienna, Austria;* ⁴*Laboratory for Ion Beam Physics, ETH-Zurich, CH-8093 Zurich,
Switzerland*

(Manuscript received 15 October 2010; in final form 2 May 2011)

ABSTRACT

We investigated the variability of ^{210}Pb , ^7Be and ^{10}Be in coastal Antarctic aerosol samples based on continuous, monthly and annually resolved time series obtained from Neumayer Station over the period 1983 to 2008. Clear seasonal cycles peaking in the local summer half year stand out as a common feature of all three radionuclide records. Time series analyses suggest that significant multiannual changes are confined to a 4–6 yr periodicity resembling that of the Southern Annual Mode index in case of ^{210}Pb and to the expected decadal solar cycle in case of the cosmogenic Be-isotopes. Both, changes in the meridional transport and surface inversion strength appear to drive the seasonal ^{210}Pb cycle, which generally peaks in November. In contrast, stratospheric air mass intrusions are proved to be the main reason for the Be-isotopes seasonality. This finding is revealed by enhanced $^{10}\text{Be}/^7\text{Be}$ ratios occurring during late summer / early autumn broadly concurrently with the individual Be-isotopes and the $^7\text{Be}/^{210}\text{Pb}$ ratio. The ^{10}Be and ^7Be records clearly reflect the decadal, solar-modulated production signal but, for unknown reasons, they substantially differ in their detailed pattern. It is ruled out, that an excess ^7Be production by solar energetic particles was responsible for this mismatch.

1. Introduction

Atmospheric records of aerosol-borne radionuclides provide important clues for investigating the sub-micron aerosol cycle. Particularly useful in this respect, are tropospheric beryllium-10 (^{10}Be) and beryllium-7 (^7Be), which are sensitive to the stratosphere/troposphere exchange (STE) and lead-210 (^{210}Pb) tracing the long-range transport of continental sub-micron aerosol. ^7Be and ^{10}Be are mainly produced by cosmic ray interactions with atmospheric nitrogen and oxygen making the lower stratosphere the major source region of these cosmogenic radionuclide (O'Brian, 1979; Masarik and Beer, 1999; Webber et al., 2007). In contrast, the relevant source region for ^{210}Pb , a long-lived decay product (radioactive lifetime $\tau = 32\text{a}$) of the terrigenous noble gas Radon-222 (^{222}Rn , $\tau = 5.5\text{d}$) is confined to the lower continental troposphere.

However, common to all these radionuclides is the fact, that after production from their atmospheric precursors they become quickly attached to the sub-micron fraction of the atmospheric aerosol (Sanak et al., 1981; Whittlestone, 1990). Thus, these radionuclides tag the secondary aerosol body which atmospheric cycle eventually governs their transport within, and their removal from the atmosphere.

Since ^7Be and ^{210}Pb can be readily analysed in high volume aerosol samples an extensive database exists from national networks focussing on atmospheric radioactivity monitoring (see e.g. EML, 2010; Kolb, 1992). In contrast to chemical aerosol species, these radionuclides are associated with relatively well-known spatio-temporal source distributions. They are widely used, therefore, for the validation of aerosol-related Chemical Transport Models (Rehfeld and Heimann, 1995; Koch et al., 1996; Barrie et al., 2001; Considine et al., 2005) where, particularly, the vertical convective mixing, the stratosphere/troposphere exchange and the aerosol removal rate remained critical issues.

Beyond global model validations, mid-to-low latitude studies of atmospheric ^7Be were mainly aimed at detecting subsidence

*Corresponding author.

e-mail: Christoph.Elsaesser@iup.uni-heidelberg.de

†Present address: CTBTO Vienna International Centre, Austria.

DOI: 10.1111/j.1600-0889.2011.00543.x

events of stratospheric air masses (see e.g. Dibb et al., 1994; Graustein and Turekian, 1996; Jordan et al., 2003; Lee et al., 2007). Applications in view of solar activity related production rate changes are relatively scarce, however, since long term, high quality observations are needed for this purpose (see e.g. Aldahan et al., 2008; Hötzel et al., 1991). ^{210}Pb -based investigations mainly addressed the vertical aerosol mixing within mountain areas (Hammer et al., 2007; Lee et al., 2007), the dissection of continental versus marine air masses (Paatero et al., 2003) and the long-range transport of continental aerosol over remote marine areas (Dibb et al., 1997).

Atmospheric records of ^7Be , ^{10}Be and ^{210}Pb observed at polar ice sheets locations are particularly useful since past changes of the atmospheric aerosol load are essentially archived in the ice. ^{210}Pb and the cosmogenic radionuclide ^{10}Be deposited alongside with the chemical aerosol species may be analysed in ice cores to infer their long term atmospheric changes as well as to study the involved air/firm transfer of aerosol species. ^{10}Be is mainly distinguished from ^7Be by its much longer radioactive lifetime (2.0×10^6 a (Korschinek et al., 2010) versus 77 d in case of ^7Be) which allows deploying ^{10}Be for the ice core-based long-term reconstructions of solar activity changes (e.g. Raisbeck et al., 1981; Beer et al., 1988; Muscheler et al., 2007). However, this attempt is hampered by meteorological and depositional noise (Webber and Higbie, 2010) calling for a better understanding of the governing air/firm transfer processes. In this context, decadal-scale atmospheric observations of (cosmogenic) radionuclides are needed at ice sheet locations.

Such long term atmospheric observations of ^7Be and ^{210}Pb only exist from Antarctic sites, while several multiannual records from the Greenland Summit station were obtained year round by Dibb (2007) for that purpose. The longest Antarctic ^7Be record is available over the years 1970–1999 from South Pole (EML, 2010). It is supplemented by a 19 yr ^{210}Pb record starting in 1974. Koch and Mann (1996) evaluated this ^7Be data set in their global ^7Be study though its inhomogeneity is substantial (including frequent data gaps, systematic changes, and, in case of ^{210}Pb , high analytical uncertainties of up to several 100%). Much shorter year round records of both nuclides exist from coastal sites as Mawson, Palmer, Base President Frei, Marsh Station (all included in the EML (2010) data set), and from the French Dumont d'Urville (DDU) Station (Sanak et al., 1985). Regarding atmospheric ^{210}Pb , the latter site provides the longest record covering the 1960–1986 period (Lambert et al., 1990). A quantitative comparison of these less well calibrated α -spectrometry data with the now commonly obtained γ -spectrometry results is somewhat hampered, however.

At the coastal Antarctic Neumayer (NM) Station we started quasi-continuous ^7Be and ^{210}Pb observations in March 1983 (Wagenbach et al., 1988). They constitute the only long-term Antarctic records taken simultaneously with ionic aerosol species (Savoie et al., 1992; Wagenbach, 1996; Weller et al., 2006). Our former application of these radionuclide data con-

cerned, among others: (i) the identification of stratospheric air masses associated with changes of radiocarbon (Levin et al., 2009), volcanic sulphate (Legrand and Wagenbach, 1999), nitrate (Wagenbach et al., 1998) and reactive nitrogen oxides (Weller et al., 2002) as well as (ii) estimates regarding the fraction of continental sulphate (Minikin et al., 1998) and nitrate (Wagenbach et al., 1998) of the Antarctic surface aerosol.

Covering actually more than 25 yr, the ^7Be and ^{210}Pb records are now sufficiently long for evaluating the “local climatology” of these radionuclides. This attempt is essentially an extension of the accompanying paper by Weller et al. (2011) dealing with the NM climatology of the ionic aerosol species. Moreover, we supplemented the ^7Be data by continuous ^{10}Be -analyses over the whole period, though at much lower temporal resolution. In discussing the long-term radionuclide records we address their characteristic seasonal, multiannual and decadal variability by dedicated time series analysis (also including interlinks among the radionuclides). We emphasize here the seasonal variability, which was already investigated in detail for the ion records from NM but not for the radionuclides. Where feasible, we address the question to what extent the radionuclide variations might be associated with meteorological and source related forcing, respectively.

2. Methods

2.1 Site description and sampling

For the present paper the following characteristics on the Antarctic Neumayer sampling station are directly relevant: (i) its position at $70^\circ 39' \text{S}$, $8^\circ 15' \text{W}$ on the Ekström ice shelf some 10 km inland from the ice edge and thus only about 42 m a.s.l., (ii) a relatively high mean annual wind speed of 8.9 m s^{-1} with dominating easterly winds carrying only a moderate katabatic component. Following König-Langlo et al. (1998), only about 20% of the wind directions are associated with air masses advection from south, (iii) the mean annual net accumulation of around 30 cm (water equivalent) showing no distinct seasonal cycle and (iv) the typical range in the seasonal air temperatures of roughly -25 to -5°C . Altogether, we may expect from this ground level situation relatively intensive aerosol scavenging year round, a low persistency of strong surface inversions and a relatively weak influence of inland air masses.

A detailed evaluation of the NM meteorology is given by König-Langlo et al. (1998) while the sampling techniques of the high volume aerosol filters are reported by Wagenbach et al. (1988) and Weller et al. (2008) as well as in the accompanying paper by Weller et al. (2011). In brief, aerosol was continuously collected on (pre-cleaned) double Cellulose filters over periods ranging from a few days to several weeks (typically 14 d), which correspond to air sample volumes between 3000 and 50 000 standard cubic metre (SCM). While from March 1983 until February 1991 these filters were used for both,

radionuclide as well as chemical analyses, separate (but identical) high volume sampling systems were deployed afterwards.

2.2 Radionuclide analyses

The γ -spectrometric quantification of the ^7Be and ^{210}Pb activities detailed by Wagenbach et al. (1988) remained essentially unchanged, except regarding upgrades and renewal of the detector systems at the Institut für Umweltphysik (IUP) laboratory. ^{210}Pb samples collected before March 1985 were analysed by α -spectrometry of its decay product ^{210}Po and afterwards by γ -spectrometry. This change of the detection method did not produce any notable, systematic difference of the ^{210}Pb results. The overall relative uncertainties of the atmospheric ^{210}Pb and ^7Be activities comprising counting statistics, detector efficiency calibration and air volume determination are typically 5–10%. Due to the strongly variable fraction of ^7Be that already decayed between sampling and assay, the ^7Be uncertainties may reach in some cases up to 30%. All these analytical uncertainties do not substantially influence the radionuclide records since they are by a factor of 2–5 smaller than the natural (1σ) variability.

In contrast to the non-destructive γ -spectrometry of ^{210}Pb and ^7Be , ^{10}Be was extracted from filter aliquots for subsequent accelerator mass spectrometry (AMS) analyses. Since a relatively large effort is needed here, we had to limit the number of ^{10}Be analyses to 156, which is a factor five less than the total ^7Be data. We selected filters for the ^{10}Be analyses as to cover the whole observational period but at expense of the temporal resolution. As a result, the temporal coverage of our ^{10}Be results range from single filter (of several days) to composite annual samples. For half year or annual mean ^{10}Be analyses we pooled the single filter aliquots in order to obtain sampling intervals roughly centred at the maximum of the seasonal ^{10}Be cycle.

The target preparation for ^{10}Be AMS analyses performed at the Heidelberg laboratory comprised: (i) adding of ^9Be spike to the filter aliquots followed by acid leaching supported by ultrasonic treatment which ensured an almost total extraction of the cosmogenic Be nuclides, (ii) subsequent radiochemical Be separation as $\text{Be}(\text{OH})_2$ and production of the final BeO targets according to the standard procedures described by Wagner (1998) and Stone et al. (2004), respectively. AMS analyses were performed at the ETH-Zürich AMS-facility for samples collected before 2001 (see e.g. Kubik and Christl, 2010) and afterwards at VERA Laboratory of the University of Vienna (Priller et al., 2004; Auer et al., 2007). Respective, relative, statistical uncertainties of the AMS analyses are in the order of 4%, which is comparable to the (typical) statistical counting errors of our γ -spectrometry analyses.

2.3 Data reduction and time series analysis

We reduced the raw atmospheric ^7Be and ^{210}Pb data as to obtain quasi-continuous 25 yr records at monthly resolution (as done in

the accompanying paper on the ionic aerosol species by Weller et al. (2011)). The less resolved but quasi-continuous ^{10}Be data were collapsed into annual means for the evaluation of their long-term variation and, where possible, into monthly means for investigating their mean seasonal cycle. External data sets deployed for comparison were treated in an identical manner to the raw radionuclide data.

For the formal evaluation of the radionuclide variability we mainly deployed Singular Spectrum (SSA) and Wavelet Analysis. Given that it is quite challenging to detect an effective decadal cycle in a 25 yr time series, Monte Carlo SSA (MC-SSA) was found to be well suited to extract such information from short and noisy time series. This method is widely used to identify modulated (harmonic or non-harmonic) oscillations in climatic time series (Broomhead and King, 1986; Vautard and Ghil, 1989; Ghil et al., 2002). It is capable of decomposing the given data set into several components of interest like the 11 yr production signal in case of the monthly ^7Be time series. Aimed at assessing the significance of the SSA findings we extended the method by a Monte Carlo approach following Allen and Smith (1996). Thereby, the statistical significance is estimated against red noise (being a characteristic feature of geophysical time series). Since climate time series are rarely stationary in time we backed-up the SSA evaluation with a basic wavelet analysis which is an ideal tool for detecting localized intermittent periodicities. Here, we aimed at investigating the time behaviour of common periodicities rather than to contrast the findings of the SSA with quantitative wavelet results. We applied for this purpose the code offered by Grinsted et al. (2004) which is based on Torrence and Compo (1998). Following the latter authors, the selection of the wavelet function is not critical with regard to the qualitative results; we refer here to the instructions of Grinsted et al. (2004).

These present time series analyses essentially coincide with those of the accompanying paper by Weller et al. (2011) dealing with ionic aerosol species. However, since the seasonal cycles of the radionuclide data are less dominant (and thus not that obvious) compared to the source driven ion cycles we did not a priori skip the seasonal variability by calculating monthly anomalies. Only where needed, we eliminated the seasonal cycle, which was done by dividing each monthly value by the respective overall monthly mean.

2.4 Adoption of auxiliary Neumayer time series

From the meteorological data observed at the NM Meteorology Observatory, we derived indices which are expected to be associated with the radionuclide variability as including: (i) the precipitation pattern based on the daily fresh snow event frequency (also considering a possible snow drift bias), (ii) the vertical air mass exchange intensity between the boundary layer and the free troposphere as parametrized by the surface inversion strength and, (iii) the (thermal) tropopause height. The two latter indices are

based on the evaluation of NM radiosonde temperature profiles as detailed in the Supporting Information. Where reasonable, we used the Southern Annular Mode (SAM also denoted as AAO) and the Southern Oscillation Index (SOI) circulation indices, both adopted from NOAA Earth System Research Laboratory (2010). In addition, the neutron flux monitored at the Antarctic McMurdo Station (Bartol Research Institute, 2010) was used as proxy for the cosmic ray induced production rate change of the Be-isotopes.

3. Results

3.1 Data presentation

Figure 1 illustrates the monthly means of ^7Be and ^{210}Pb over 1983–2008. As already emphasized by a simple Gaussian low pass filtering, the seasonal signal stands out in both radionuclides records next to multi-annual changes. The latter include a decadal cycle in case of ^7Be and ^{10}Be . This behaviour may be expected from the 11-yr solar modulation of the cosmic rays induced production of these radioisotopes (i.e. Schwabe cycle). Note that in contrast to ^7Be , ^{10}Be is impaired by irregular subsampling allowing evaluation of its long-term changes on annual resolution only. Comparison of the atmospheric ^7Be and ^{210}Pb records at NM with those from other Antarctic sites revealed the following features (see also the respective data statistics summarized in Table 1 and 2):

(1) There are quite similar atmospheric levels at South Pole and NM for both radionuclides, which, in case of ^7Be , is surprising in view of the altitude and latitude differences between the sites. The temporal coverage of South Pole data is rather inhomogeneous, however (see respective illustrations in Koch and Mann (1996)). Particularly in case of ^{210}Pb , these data are

confused by a notable drop after 1984 leading to a mean level persistently lower by more than a factor of two.

(2) At the coastal sites Palmer and Marsh located north of NM at the Antarctic Peninsula (EML, 2010), mean atmospheric ^7Be and ^{210}Pb activities are lower by a factor of 3–4 and 2–3, respectively. This finding may be expected in view of the more effective aerosol scavenging at these northward positions. Moreover, in case of ^7Be , it confirms the relative minimum concentrations at this latitude associated with a low stratospheric air mass influence in the sub-Antarctic belt predicted by Stohl and Sodemann (2010). On the other hand, the coastal sites Mawson and Dumont D'Urville (DDU), which are strongly influenced by katabatic flow (Gras, 1993; König-Langlo et al., 1998) through their position at the Antarctic ice sheet edge, show the highest Antarctic ^7Be levels. However, assessing the differences between NM and other coastal ^7Be records were difficult since at the latter sites systematic analytical artefacts may not be excluded. This concerns e.g. the use of on site γ -spectrometry at DDU at very low energy resolution (Sanak et al., 1985) and the EML data being frequently below detection limit probably biasing the mean ^7Be level high. Regarding ^{210}Pb , the Mawson and NM means are virtually the same as is the ^{210}Pb level at DDU obtained by in situ gross- α counting (Lambert et al., 1990).

The NM records show a significant correlation between monthly ^7Be and ^{210}Pb data (correlation coefficient $r = 0.47$, $p < 0.005$) which is due to their broadly common seasonal cycles and the large intersample variability likely associated with meteorological changes affecting both species. This covariation increases to $r = 0.63$ at annual resolution implying that there is also a common, inter-annual influence on the atmospheric activity of these radionuclides, even though their source distributions are largely different.

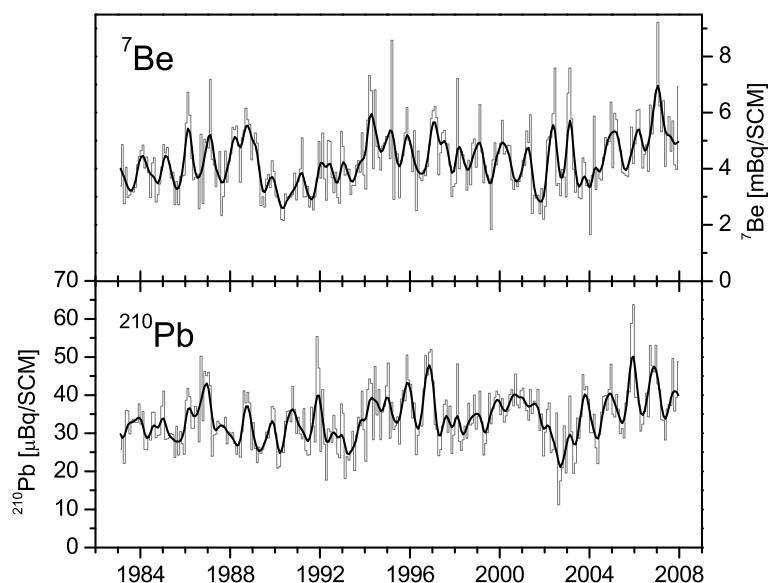


Fig. 1. Atmospheric records of ^7Be and ^{210}Pb observed at the coastal Antarctic Neumayer Station. Individual date (in grey) refer to monthly means, the thick line obtained by Gaussian smoothing highlights the seasonal cycles but reduces the true amplitudes by approx. 27%.

Table 1. Monthly data based comparison of the atmospheric ^7Be level at Neumayer with those observed at South Pole and at the coastal Antarctic Mawson Station ($67^\circ 36' \text{S}$, $62^\circ 53' \text{E}$), Palmer Station ($64^\circ 46' \text{S}$, $64^\circ 4' \text{W}$), Marsh Station ($62^\circ 11' \text{S}$, $58^\circ 59' \text{W}$) and Dumont D'Urville ($66^\circ 40' \text{S}$, $140^\circ 01' \text{E}$). In order to reduce the inhomogeneities in the monthly EML data (including zero and overshooting outliers) values being a factor of 5 above and below the medians, respectively are discarded

	Period	Mean (median) ^7Be [mBq/SCM]	Relative SD (%)	Min. – max. ^7Be [mBq/SCM]
Neumayer (this study)	1983–2008	4.3 (4.1)	27	1.7–9.2
South Pole (EML, 2010)	1970–1999	4.2 ^a (3.7)	49 ^a	(1.1–11.3) ^a
Mawson (EML, 2010)	1987–1993	5.4 ^a (4.6)	39 ^a	(2.3–14) ^a
Palmer (EML, 2010)	(1990–1993) & (1995–1999)	1.3 ^a (1.2)	37	0.5–2.8
Marsh (EML, 2010)	(1990–1993) & (1996–1999)	1.4 ^a (1.2)	35 ^a	(0.3–2.7) ^a
Dumont d'Urville (Sanak et al., 1985)	1978–1981	6.8 (6.6)	20	4.8–9.7

^aData set reduced with respect to outliers, except for medians, see caption.

Table 2. Same as Table 1 but for ^{210}Pb

	Period	Mean (median) ^{210}Pb [$\mu\text{Bq/SCM}$]	Relative SD (%)	Min. – max. ^{210}Pb [$\mu\text{Bq/SCM}$]
Neumayer (this study)	1983–2008	34 (33)	23	11–64
South Pole (EML, 2010)	(1974–1976) & (1981–1999)	36 ^a (29)	65 ^a	(6–142) ^a
Mawson (EML, 2010)	1987–1993	30 ^a (28)	33 ^a	(10–59) ^a
Palmer (EML, 2010)	1990–1999	15 ^a (13)	46	(4–30) ^a
Marsh (EML, 2010)	(1990–1993) & (1994–1999)	17 ^a (15)	44	(4–47) ^a
Dumont d'Urville (Lambert et al., 1990)	1960–1986	– (30 ^b)	–	–

^aData set reduced with respect to outliers, except for medians, see caption.

^bObtained by visual inspection of fig. 2 in Lambert et al. (1990).

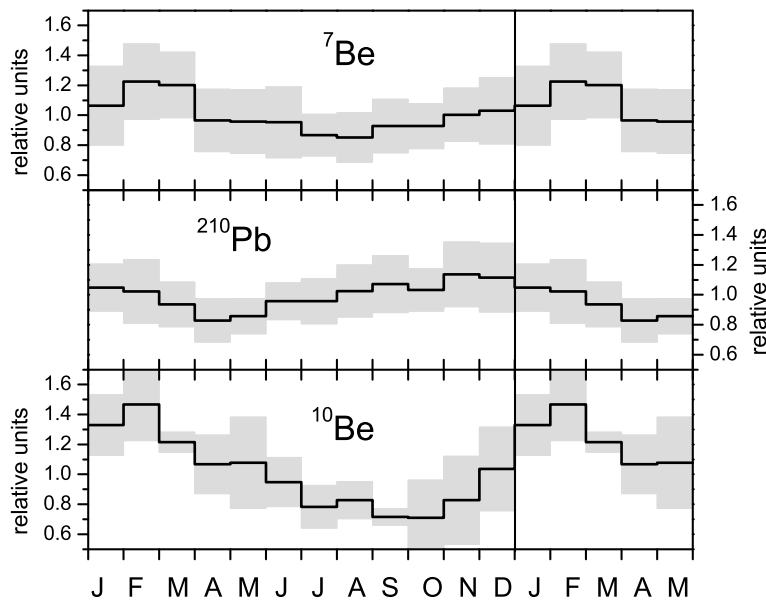


Fig. 2. Mean seasonal radionuclide cycles observed at Neumayer over the period 1983 to 2008 for ^7Be and ^{210}Pb and (1983–1986) & (1990–1991) for ^{10}Be . Displayed monthly values refer to relative stacked, deviations from the multi-annual trend (calculated by Gaussian smoothing). Grey areas indicate the 1σ variability.

Figure 2 displays the mean seasonal cycles of ^7Be , ^{10}Be and ^{210}Pb , which were simply compiled by stacking the relative deviations of the monthly means from the individual long-term patterns (estimated by Gaussian smoothing). An enhanced atmospheric level during the local summer half year is seen for all

three species. Their seasonal patterns are somewhat different, however. We found for ^7Be and ^{10}Be relative seasonal excursions of around 22% and 47% (both upward during summer), respectively which are higher than those of ^{210}Pb (18%, downward during winter). Note, that the much lower time coverage

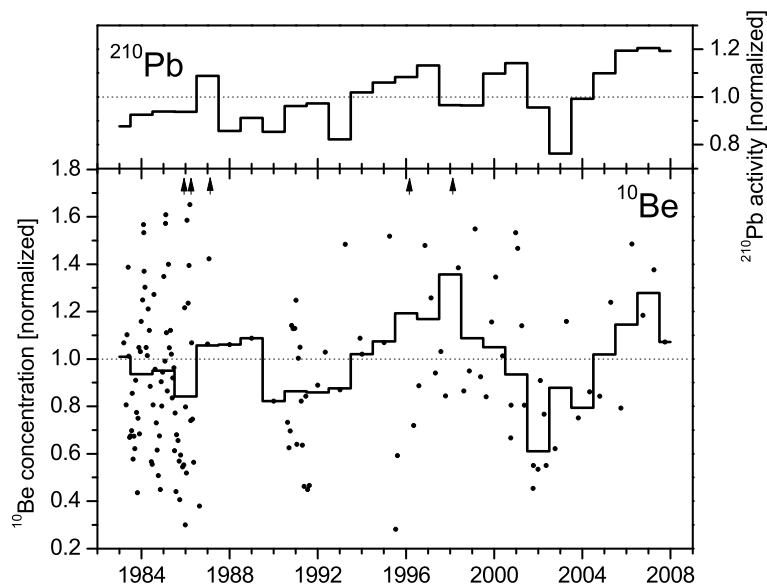


Fig. 3. Long term changes of annual mean ^{10}Be and ^{210}Pb at Neumayer normalized to respective overall means: ^{210}Pb : $34 \mu\text{Bq/SCM}$, ^{10}Be : 4.6×10^4 atoms/SCM. Individual ^{10}Be data are indicated by dots centred at mid-point sampling intervals ranging between a few days and 1 yr, arrows denote out of scale data of up to 2.9.

of ^{10}Be data may partly add to the slightly different pattern of the ^7Be versus the ^{10}Be cycle. Overall, the seasonal Be isotopes change lags the ^{210}Pb cycle (generally peaking in November) by 3 months.

Common to all time series are weakly increasing trends over the observational period. While for monthly ^7Be and ^{210}Pb data a formally significant, linear trend of $0.8\text{--}0.9\% \text{ yr}^{-1}$ is obtained the slightly weaker trend of annual ^{10}Be ($0.4\% \text{ yr}^{-1}$) remains insignificant (see Fig. 3). For details on the testing procedure, see accompanying paper by Weller et al. (2011). In case of the Be-isotopes, the relevance of these findings is hard to assess since the decadal production mode is embedded in their 25 yr trends. Interestingly, neutron monitor count rate at McMurdo reveals a slightly positive trend during that period ($0.2\% \text{ yr}^{-1}$). Overall, we conclude that the long-term radionuclide trends are so low that they might result from a systematic analytical artefact as well.

3.2 Time series decomposition

Aimed at revealing the annual to decadal variability of the ^{210}Pb and ^7Be records we decomposed the de-trended monthly data by SSA and estimated the significance of these components by the Monte Carlo–SSA method. Different realizations of the SSA procedure by using varying adjustments of the controlling parameter (for details of the SSA application, see Supporting Information) revealed the following significant components: (i) a seasonal cycle and a 4–6 yr oscillation in the ^{210}Pb record and, (ii) in case of ^7Be , a seasonal and a decadal cycle as well as a notable 2–3 yr oscillation which is not significant, however, on the 95% confidence level. While the selected SSA parameter was found to have a relatively small impact on the above findings, it may substantially influence the decomposition qual-

ity of the significant signals. Hence, the quantitative analysis of amplitudes and explained variance of the concerned signals are depending to some extent on the deployed SSA parameter. In the present case, variation of the parameter results in a trade off between the amplitude modulation (associated with shared variance of the filtered components) and a clear separation of the significant components (i.e. deploying more harmonic components). However, for the wide range of tested SSA parameter adjustments we found that the seasonal cycle dominates both data sets in view of the explained variance of the time series. Figure 4 illustrates the results for a SSA window length of $M = 90$ (months) which allowed for a reasonable separation of the seasonal and the multi-annual oscillations. However, the SSA method might underestimate their amplitude modulation, in the present case.

For the extraction of multi-annual oscillations, we eliminated the seasonal cycle before SSA, which makes the separation of the multi-annual from the seasonal signal a less critical issue. In case of ^7Be , we restricted the lower SSA window length to 40 in order to achieve a clear separation of the ambiguous 2–3 yr mode from the decadal cycle while the upper boundary was limited to 100. Regarding the decadal ^7Be cycle, we found that both maxima are lying within the range of 10–15% above the overall mean, while the two minima differ as lying below that mean by 15–22% in the first and 5–10% in the second observational period, respectively. For sake of comparability, we applied the same SSA parameter range for the ^{210}Pb time series analyses. This revealed relative amplitudes of the 4–6 yr ^{210}Pb cycle of approximately 2–12% in the first and 10–20% in the second half of the record.

Wavelet Analyses results which are detailed in the Supporting Information confirm the above findings and, moreover, illustrate that the signals are not stationary in time. Interestingly, the

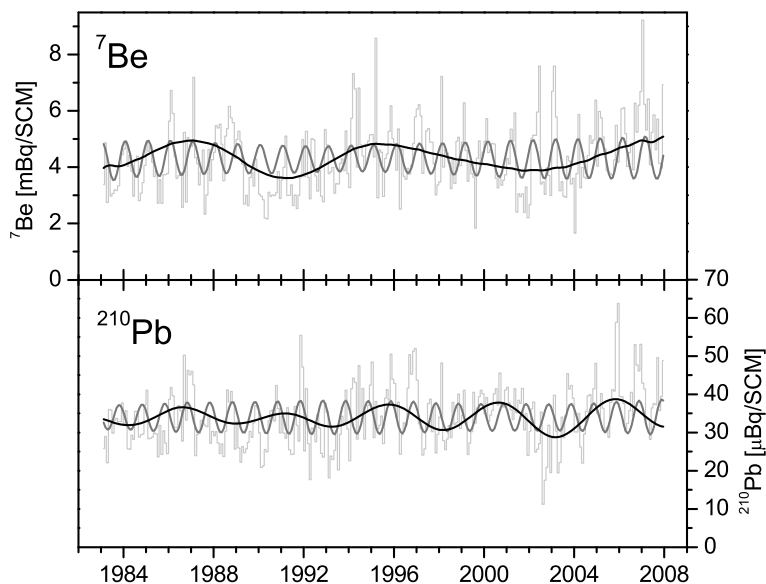


Fig. 4. (Monte Carlo) Singular Spectrum Analysis of Neumayer radionuclide time series using a window length of $M = 90$ (months). Displayed are the significant first plus second EOF components (i.e. seasonal mode) and the third plus fourth one (i.e. multiannual to decadal mode) together with the original monthly means (thin grey line). Explained variance of shown components with respect to original monthly means are estimated at: 17% and 15% for the seasonal and decadal ${}^7\text{Be}$ cycles, as well as 17% and 13% for the seasonal and 4–6 yr ${}^{210}\text{Pb}$ oscillations, respectively.

periods with particularly distinct seasonal signals are different for ${}^7\text{Be}$ and ${}^{210}\text{Pb}$, respectively: For ${}^7\text{Be}$, the seasonality tends to be especially pronounced during 1985–1987 and 2000–2002, whereas for ${}^{210}\text{Pb}$ this holds during 1995–1997 and 2004–2007. Inspection of the multi-annual signals in Fig. 4, reveals that the 4–6 yr ${}^{210}\text{Pb}$ cycle appears to be more pronounced in the second half of the record, while the decadal cycle of ${}^7\text{Be}$ shows up more distinct in the first section. Respective wavelet results are shown in the Supporting Information, but note, that within our 25 yr record length oscillations with periods exceeding approximately 10 yr may not produce meaningful results. We may conclude, that the time series analysis of the ${}^7\text{Be}$ and ${}^{210}\text{Pb}$ monthly mean records clearly reveals a dominant seasonal cycle on top of a significant multiannual oscillation. Relative amplitudes of the latter vary with time and do not significantly exceed 20% of their overall mean.

4. Discussion

4.1 ${}^{210}\text{Pb}$ variability

4.1.1 *Seasonality.* As addressed in Section 3, the atmospheric ${}^{210}\text{Pb}$ variability at NM is evidently dominated by the seasonal cycle. Processes responsible for this finding may comprise: (i) local changes, including vertical air mass exchange with the free troposphere and precipitation scavenging, (ii) large scale effects, associated with the meridional long range transport and aerosol removal en route and (iii) seasonal changes in the continental source region, including deep vertical mixing and precipitation scavenging as well as, though almost negligible, changes in the continental radon exhalation rate (Dörr and Münnich, 1990).

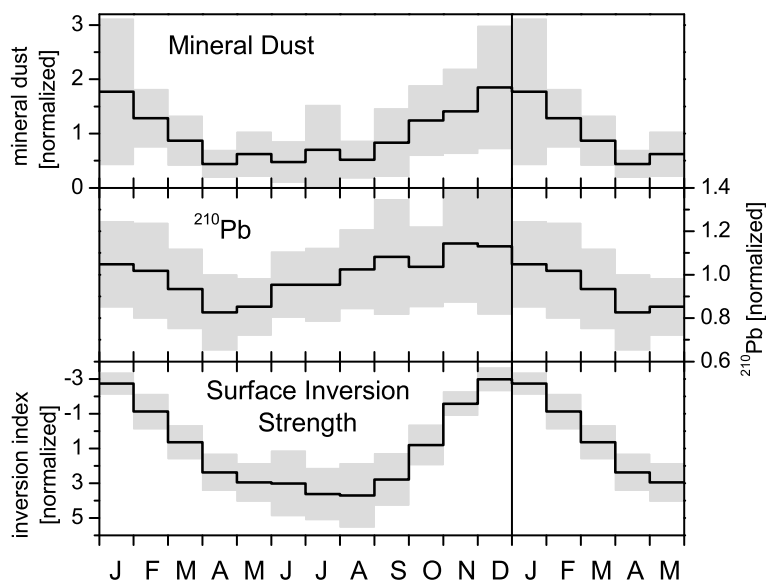
Regarding local effects, we may neglect the seasonal change of local snow scavenging since the accumulation rate at NM does

not significantly vary with season. On the other hand, we found that the strength of the surface temperature inversion shows a clear seasonal pattern being typically in antiphase with the ${}^{210}\text{Pb}$ cycle (see Fig. 5). This behaviour may be expected since the inversion strength is associated with the renewal rate of the boundary layer air (being depleted in ${}^{210}\text{Pb}$). Since strong surface inversions persist at inland positions, particularly during winter a higher seasonal ${}^{210}\text{Pb}$ amplitude should be seen here. Indeed, compared to NM, ${}^{210}\text{Pb}$ (and ${}^7\text{Be}$) records at South Pole show enhanced seasonal amplitudes. This difference is mostly due to the comparably lower winter levels at the inland site.

Comparing at NM the seasonal ${}^{210}\text{Pb}$ pattern with that of mineral dust (Weller et al., 2008), revealed that both species peak during the local summer half year. Compared to ${}^{210}\text{Pb}$, the summer/winter contrast of the mineral dust component is larger, however, by a factor of four, approximately (see Fig. 5). Noting the substantial difference between the secondary ${}^{210}\text{Pb}$ particles derived at a constant rate from the ${}^{222}\text{Rn}$ volume source and the primary mineral dust particles emitted (at variable strength) by the continental surface makes this comparison inconclusive for depicting the main driver of the seasonal ${}^{210}\text{Pb}$ cycle (i.e. local inversion strength versus long range transport changes). Nevertheless, the much smaller seasonal ${}^{210}\text{Pb}$ amplitude compared to mineral dust may be expected due to the significantly higher atmospheric residence time of ${}^{210}\text{Pb}$. Accordingly, seasonal changes associated with the meridional transport time or with the dry deposition flux within a stable surface inversion layer would be less important for ${}^{210}\text{Pb}$. Moreover, in contrast to mineral dust, the minimum atmospheric ${}^{210}\text{Pb}$ level in Antarctica is determined by the ${}^{222}\text{Rn}$ inventory of the south polar troposphere (as partly compensating the ${}^{210}\text{Pb}$ removal).

In Antarctica, the atmospheric ${}^{222}\text{Rn}$ activity is believed to mainly depend on the typical transit time from the

Fig. 5. Mean seasonal cycles of mineral dust, ^{210}Pb , and strength of surface inversion layer observed at Neumayer. All data are displayed relative to the overall mean with shaded areas indicating the one σ range. Mineral dust refers to the Lanthan record reported by Weller et al. (2008) over the period 1999 to 2003 which provides the most comprehensive crustal element data set from this site. The inversion strength index increases downwards and essentially refers to the observed temperature gradient (for details see Supporting Information).



continental source regions (Heimann et al., 1990). At NM, it regularly exhibits a maximum between December–March (not shown) exceeding on a monthly basis, the overall mean by 50% approximately. Within the local summer months showing enhanced ^{222}Rn also ^{210}Pb and mineral dust have their annual maximum. On first sight, this observation would suggest that in addition to near surface vertical mixing also the efficiency of the meridional long-range transport might be decisive for the observed ^{210}Pb seasonality.

However, we may not neglect the oceanic ^{222}Rn source at coastal Antarctica whose relative contribution at NM was simulated by Heimann et al. (1990) to account for 40%, on average. Thus, the ocean derived ^{222}Rn expected to peak during the local sea ice minimum (around February) might have biased the seasonal ^{222}Rn cycle towards higher levels in late summer. This prevents us actually from using our NM ^{222}Rn record in a straightforward way for assessing the role of rapid meridional air mass exchange on the observed ^{210}Pb seasonality.

Finally addressing changes within the continental source region which might be relevant for the seasonal ^{210}Pb cycle at NM we may consider: (i) deep vertical mixing, transporting ^{210}Pb and its ^{222}Rn precursor to mid tropospheric levels from where the ^{210}Pb long range transport would be more efficient and, (ii) a strong seasonal contrast in precipitation scavenging. Inspecting the mean seasonality of atmospheric ^{210}Pb at 13 southern hemispheric sites from the EML database (covering latitudes between 16°S and 51°S and including coastal as well as inland sites) we found a seasonal maximum generally within the austral winter half year, thus opposite to the one observed at NM. We note also that the continental ^{210}Pb maximum in winter does not generally correspond to a precipitation minimum. Thus, a prominent contribution of the continental ^{210}Pb source variation to the seasonal cycle in Antarctica may be neglected on

first sight. On the other hand, the finding of an opposite ^{210}Pb cycle between mid-latitudes and NM is strictly valid only for the near surface source layer. This is because non of the investigated sites (except the tropical Chacaltaya 5220 m a.s.l. at 16°S peaking around May/June) is representative for the free or mid continental troposphere. It remains unclear, therefore, whether the seasonal ^{210}Pb (^{222}Rn) cycle at higher continental altitudes would be opposite to that obtained at the ground level sites. At least for Western Europe, we observed an opposite seasonal ^{210}Pb cycle between mountain peaks and low land sites, respectively (Hammer et al., 2007). As controlled by vertical mixing, ^{210}Pb of the higher continental troposphere should peak during the local summer half year, hence, broadly in phase with the Antarctic ^{210}Pb maximum.

Tentatively excluding substantial seasonal changes in the ^{210}Pb (^{222}Rn) source strength we may conclude that the seasonal ^{210}Pb cycle at NM is most likely controlled by a combination of the local change in the surface inversion persistency and the large scale effect associated with the seasonality in the meridional long range transport efficiency. It is not possible at this stage to disentangle the relative importance of these drivers for the seasonal ^{210}Pb signal. Evidently, both effects encompass a whole suite of meteorological influences, which vary on the multi-annual time scale as well (though at less extent). We may expect therefore that the atmospheric ^{210}Pb variability might include also long-term changes, which are related to weather and circulation patterns. This issue is addressed, in the following section.

4.1.2 *Multiannual ^{210}Pb changes.* The SSA evaluation of the NM ^{210}Pb record revealed in addition to the obvious seasonal cycle only an apparent 4–6 yr mode as a formally significant feature. Variability within this frequency range is quite common for the Antarctic circulation pattern (e.g. Jacobs and Mitchell,

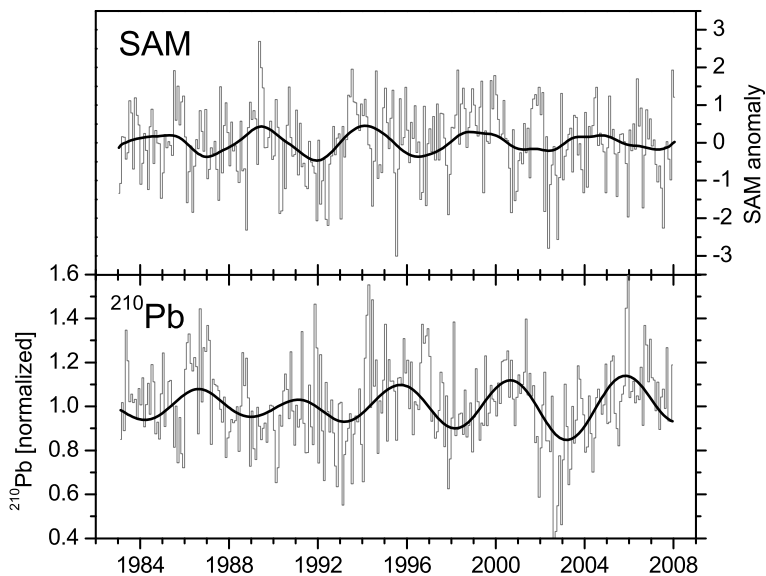


Fig. 6. Comparison of Southern Annular Mode (SAM) anomalies with de-seasonalized and de-trended ^{210}Pb record at Neumayer. Grey: monthly data, in case of ^{210}Pb normalized to the overall monthly mean; bold line: first plus second SSA (Singular Spectrum Analysis) components corresponding to a cyclicity of 4–6 yr.

1996; White and Peterson, 1996; Weller et al., 2011). This meteorological phenomenon may influence ^{210}Pb at NM on the large scale (via transport and degree of scavenging) as well as locally via the meteorological conditions governing the surface inversion property. We extended, therefore, the SSA time series analyses applied for ^{210}Pb to the Southern Annual Mode (SAM) and the Southern Oscillation (SOI) indices as well as to local meteorological parameters (see Supporting Information for these auxiliary records). We found significant periodicities on the 4–6 yr scale in the SAM and SOI indices as well as in the snow event frequency, the de-seasonalized temperature and the boundary layer inversion strength. Figure 6 shows the typical SSA results for ^{210}Pb and SAM. Phase-lag correlation analysis reveals that ^{210}Pb lags the SAM signal by 18 months, approximately. Attribution of causes for this feature would be rather complex, since they may include large scale as well as local effects. In assessing the relevance of the entirely formal ^{210}Pb -SAM link, we investigated the correlations of annual as well as of de-seasonalized monthly ^{210}Pb data with local meteorological indices (including the inversion strength index). As expected, the inversion index is clearly anticorrelated to the snow event frequency, temperature and wind speed (for annual as well as de-seasonalized monthly means). However, among these local meteorological parameters, none show a significant correlation with ^{210}Pb . Hence, on the local scale we could not identify a main driver for the multiannual ^{210}Pb variability.

4.2 Be-isotopes

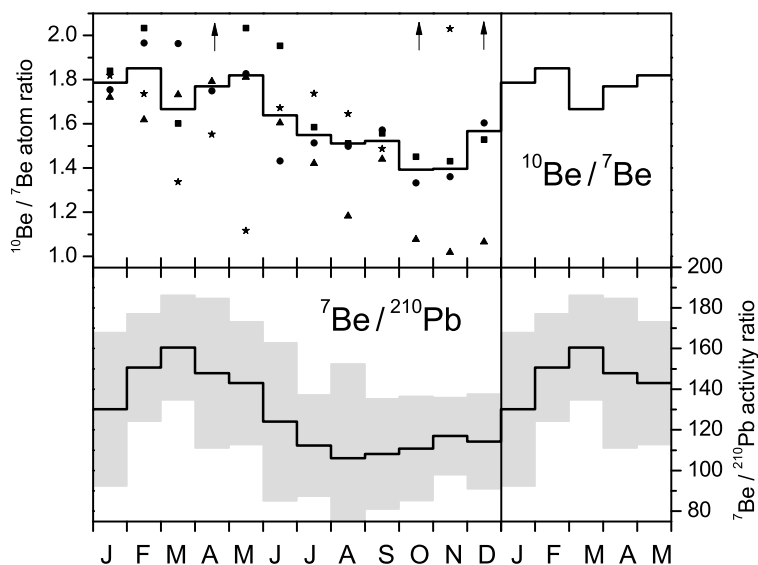
4.2.1 Seasonality. In assessing the seasonal cycles of ^7Be and ^{10}Be shown in Fig. 2, it is important to consider that the source strength (and thus the atmospheric concentration) of these radionuclides strongly increases with height and peaks in the lower polar stratosphere where it strongly decreases towards

lower latitudes (Usoskin and Kovaltsov, 2008; Kovaltsov and Usoskin, 2010). Accordingly, the stratosphere/troposphere exchange as well as the subsidence of mid to high tropospheric air may shape the seasonal cycle of the Be-isotope records at NM (in addition to the surface inversion strength and meridional air mass transport already addressed in case of the ^{210}Pb seasonality). The typical three months by which the seasonal cycles of Be-isotopes lags the ^{210}Pb one, likely reflect the obvious spatial contrast in the source distribution of these radionuclides (note that their cosmogenic as well as their terrigenous source strength shows almost no seasonal change). The seasonal amplitude of ^{10}Be exceeds that of ^7Be by a factor two, approximately (see Fig. 2). This observation reflects the higher stratosphere/troposphere contrast of ^{10}Be (vs. ^7Be) and implies that tropospheric ^{10}Be concentrations are more sensitive to stratosphere air mass intrusions. As outlined below, this effect emerges since a good deal of ^7Be (but not ^{10}Be) already decays in the stratosphere.

It remains to address to what extent cross tropopause air mass transport (and subsequent subsidence in the troposphere) may drive the seasonal Be-isotopes cycles. We used for this purpose the $^7\text{Be}/^{210}\text{Pb}$ and $^{10}\text{Be}/^7\text{Be}$ ratios, which should partly eliminate the influence related to the surface inversion changes or strong precipitation events (Fig. 7). Indeed, the relative variability of the monthly $^7\text{Be}/^{210}\text{Pb}$ and $^{10}\text{Be}/^7\text{Be}$ data is reduced by around 40% relative to what is expected from formal error propagation based on the single isotope data variations. Unlike for $^7\text{Be}/^{210}\text{Pb}$, there is a straightforward interpretation of the $^{10}\text{Be}/^7\text{Be}$ ratio. Following Raisbeck et al. (1981), this ratio may be expressed for an isolated, well-mixed atmospheric box at equilibrium between production and removal rates as

$$\frac{^{10}\text{Be}}{^7\text{Be}} = \frac{P_{10}}{P_7} \left(1 + \frac{\tau_a}{\tau_7} \right). \quad (1)$$

Fig. 7. Mean seasonal cycle of the radionuclide ratios (atoms/atoms) $^{10}\text{Be}/^7\text{Be}$ and $^7\text{Be}/^{210}\text{Pb}$ (Bq/Bq) at Neumayer. Observational periods (1983–1986) and (1990–1991) for $^{10}\text{Be}/^7\text{Be}$ and 1983–2008 for $^7\text{Be}/^{210}\text{Pb}$. For illustration of the $^{10}\text{Be}/^7\text{Be}$ data variability, individual data points are shown as attributed to the different annual cycles: (■) 1983/1984, (●) 1984/1985, (▲) 1985/1986 and (★) 1990/1991. Arrows indicate out of scale data of up to 2.8. The grey band denotes the 1σ scatter of the individual monthly means $^7\text{Be}/^{210}\text{Pb}$ data.



Here, P_{10} and P_7 denote the ^{10}Be and ^7Be production rates, respectively (assumed to be temporally and spatially constant), τ_7 the radioactive lifetime of ^7Be (77d) and τ_a the atmospheric residence time of the relevant aerosol within the considered box. In this simplistic case, $^{10}\text{Be}/^7\text{Be}$ depends only on τ_a and increases linearly with τ_a (since the radioactive decay of ^{10}Be is negligible). Thus, given $P_{10}/P_7 = 0.52$ (Masarik and Beer, 2009) we would expect that this ratio is about 3 in the stratosphere (taking there $\tau_a \approx 15$ months), drops to 0.73 in the free troposphere ($\tau_a \approx 30$ d) if no STE is assumed and would come close to the production ratio within the surface boundary layer ($\tau_a \approx 10$ d). Obviously, the $^{10}\text{Be}/^7\text{Be}$ ratio at NM remains always above the apparent tropospheric equilibrium value (see respective seasonal cycle displayed in Fig. 7). This implies a year round influx of stratospheric air being particularly substantial in late summer. During that season, we observed a $^{10}\text{Be}/^7\text{Be}$ ratio of around 1.9, which is significantly higher than the local winter spring value of around 1.4. Following Dibb et al. (1994) and Wagenbach (1996), these ratios broadly translate into a stratospheric ^{10}Be (or ^7Be) fraction seen at surface level, if the τ_a values are given for the well-mixed stratospheric and tropospheric boxes, respectively. Assuming, for example, for τ_a 15 months in the stratosphere and 1 month for the whole troposphere, we would arrive for the stratospheric ^{10}Be fraction at NM (relative to the one produced in the troposphere) at 2.6 in late summer and 1.3 in winter to spring, which makes a significant difference.

A qualitatively similar picture is obtained from the mean seasonal changes observed for $^7\text{Be}/^{210}\text{Pb}$ and for both Be-isotope concentrations. This finding indicates that their seasonal cycles are also controlled by air masses subsidence from the upper troposphere and stratosphere. We note, however, that even the $^{10}\text{Be}/^7\text{Be}$ ratio may be affected by seasonal changes of the surface inversion layer properties (e.g. lower height during winter associated with lower aerosol residence time within the sur-

face layer). However, since the temporal decline of $^{10}\text{Be}/^7\text{Be}$ within the inversion layer would be more important when the production rate or the inversion lifetime are high, the decrease of this isotope ratios within the surface layer should be of very minor importance in coastal areas.

This view is corroborated, by a snow pit study at the high accumulation Antarctic Law Dome site where Pedro et al. (2006) found a seasonal ^{10}Be cycle which pattern is consistent with our atmospheric ^{10}Be record. Since fresh snow is mainly sampling the air above the surface inversion layer, the good correspondence between the snow and aerosol data argues against inversion changes to play a dominant role for the seasonality of the atmospheric Be-isotope records, at least, in coastal areas. Particularly during winter, the surface inversion influence is expected to be more distinct at inland sites. Indeed, comparison of the ^7Be seasonality in the overlapping period at South Pole and NM point to a significantly higher summer/winter contrast at South Pole though, the overall ^7Be means are quite comparable at these sites. This spatial difference in the seasonal ^7Be amplitude is mainly governed by lower winter concentrations at South Pole compared to NM (as already seen in case of ^{210}Pb) while the summer values are only slightly higher at South Pole. This finding is corroborated by concurrent ^7Be and ^{10}Be observations we obtained over three local summer seasons at the deep drilling sites Kohnen ($75^\circ 0' \text{S}$, $0^\circ 4' \text{E}$) and Dome C ($75^\circ 6' \text{S}$, $123^\circ 20' \text{E}$) where only an enhancement by 20–50% is observed at the plateau sites versus NM (Piel et al. (2006) and unpublished IUP results).

Processes driving the seasonal cycle of the Be-isotopes (and associated ratios) may include the vertical and latitudinal air mass exchange within the (polar and mid-latitude) stratosphere and troposphere as well as the trans-tropopause transport. Even so, identification of their relative importance is outside the scope of this paper, we considered the seasonal change in the polar

(thermal) tropopause height which is inversely related to the inversion strength of the tropopause (Randel and Wu, 2010). We may expect a higher tropopause level to enhance the tropospheric inventory of the Be-isotopes during that season. However, inspection of the seasonal tropopause height cycle (obtained from NM temperature soundings) revealed that it changes in anti-phase to the observed seasonal cycle of the Be-isotopes (and related ratios). Thus, the seasonal amplitudes of the Be-records are attenuated at best, by the seasonal change of the polar tropopause height (and its associated inversion strength).

Evidently, the common seasonal maximum observed for the single Be-isotopes and the $^{10}\text{Be}/^7\text{Be}$ and $^7\text{Be}/^{210}\text{Pb}$ ratios in local summer to fall implies a maximum influence of stratospheric air during that time. This finding is in contradiction with the traditional perception of Antarctic circulation pattern (Roscoe, 2004; Holton et al., 1995 and references therein). It is also at odds with various modelling studies of the global atmospheric ^7Be (^{10}Be) cycle (see among others Brost et al., 1991; Rehfeld and Heimann, 1995). This is mainly because these simulations predict a seasonal Be-isotope cycle at SH polar latitudes peaking roughly during April-June and/or October. On the other hand, Lagrangian transport models presented by James et al. (2003) as well as Stohl and Sodemann (2010) reproduce the seasonality of the stratospheric air subsidence to the Antarctica surface in qualitative agreement with our observation at NM. Worth mentioning in this context is the excellent correspondence between the seasonal cycle of the net trans-tropopause air mass transport south of 30°S (simulated by James et al. (2003)) with those of $^{10}\text{Be}/^7\text{Be}$ and $^7\text{Be}/^{210}\text{Pb}$ at NM.

4.2.2 Decadal changes. As the production of the Be-isotopes is modulated by the solar cycle, their atmospheric variability should include a decadal variation (i.e. Schwabe sun spot cycle). However, the decadal pattern of aerosol-borne cosmogenic radionuclides cannot be clearly prescribed given the non-

stationary production distribution (Masarik and Beer, 1999, 2009; Usoskin and Kovaltsov, 2008; Kovaltsov and Usoskin, 2010), the uncertainty in their relevant transport (Stohl and Sodemann, 2010) and the complex spatial pattern of aerosol removal processes. These deficits leave the production signal of the Be-isotope records strongly embedded in meteorological noise. Nevertheless, our SSA results revealed a significant decadal change in the monthly ^7Be data, which, according to Fig. 8, is seen as well in the annual ^{10}Be record. To our knowledge, these data are the first providing a clear decadal cycle of both Be-isotopes (a somewhat shorter co-isotope record reported by Aldahan et al. (2008) from two sites in Sweden remained less clear in this respect). However, a straightforward quantification of the production signal inherent to the NM records emerged difficult.

Correlation analysis based on annual means of ^7Be and ^{10}Be with local meteorological data, neutron flux and circulation indices revealed: a clear correlation between both Be-isotopes ($r = 0.70$) and, a comparable correlation with the McMurdo neutron monitor data mainly reflecting changes in the cosmic ray flux (^7Be : $r = 0.73$; ^{10}Be : $r = 0.72$). On this multiyears time scale, the inverse relationship with the surface inversion ceased (as with all other local meteorological or circulation indices) except in case of the snow event frequency which correlates at $r = 0.62$ surprisingly well with ^7Be (though at lesser extent with ^{10}Be and ^{210}Pb). Accordingly, on the annual scale the fresh snow frequency seems to be a more useful index for comparison with the radionuclide pattern than the grand averages of the (loosely defined) surface inversion strength or of other meteorological parameters.

Already from visual inspection of the decadal Be-isotope cycles (shown in Fig. 8) we note that both species generally follow the production signal but differ significantly in the individual shape of their decadal cycles. Obviously, their correspondence

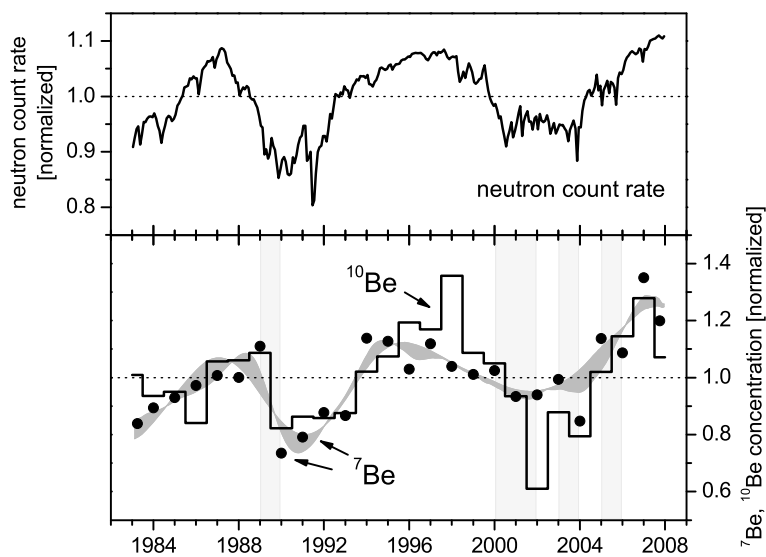


Fig. 8. Decadal cycle of atmospheric ^7Be and ^{10}Be records at Neumayer Station compared to the production signal given by monthly mean neutron count rate data from the Antarctic McMurdo Station (Bartol Research Institute, 2010). All data are displayed relative to the overall mean. The grey band reflects two limiting cases of the SSA-decomposition applied to monthly ^7Be data (see Supporting Information) to which the weak linear ^7Be trend was re-added. Annual ^7Be means are indicated by black dots centred at mid- ^{10}Be intervals. Vertical bars denote periods with strong and frequent solar energetic particle events adopted from the compilation of related production rate enhancements by Webber et al. (2007).

is not stationary as, for example, major deviations occur during the 2000–2004 solar maximum (i.e. production minimum) which shows up much more distinct in the ^{10}Be record. On the one hand, we may expect that changes in production (as well as removal) should affect both Be-isotopes in the same way. On the other, they are known to react systematically different on the regular decadal production cycle. In a global sense, ^{10}Be is expected to lag behind ^7Be by some months (which is a consequence of the much smaller stratospheric lifetime of ^7Be) whereas the difference in the relative amplitudes remains negligible. Hence, excluding an analytical artefact the feature of a partially substantial mismatch of the long term ^7Be and ^{10}Be patterns is hard to understand unless traced back to years with extreme transport anomalies or to a transient difference in the nature of the production process.

Indeed, in view of the Be-isotope production solar energetic particles (SEP) may be of concern since their contribution to the overall ^7Be production (commonly governed by galactic cosmic rays) is roughly one order of magnitude higher than for ^{10}Be (Webber et al., 2007; Masarik and Beer, 2009). While this effect is thought to be negligible on the global scale, it could be significant in polar areas, which are subject to strongly reduced geomagnetic shielding (Usoskin et al., 2009). Since SEP events likely peak during production minima the resulting increase of polar stratospheric ^7Be concentration might attenuate the amplitude of the decadal ^7Be cycle. Accordingly, Koch and Mann (1996) put the abnormal phase lag of the South Pole ^7Be record with respect to the solar cycle down to the possible impact of solar particles. We cannot confirm that perception by our NM data, where the SEP related production enhancement during 1989 (being of comparable strength as that in the early 2000 period) is not reflected in the data. Moreover, during the 2000–2004 SEP period, ^7Be fits here more closely to the galactic cosmic ray (GCR) production signal than the undershooting ^{10}Be . Although we cannot exclude any contribution of the outstanding 2000–2006 SEP events to the ^7Be level at NM, it is unlikely that the generally different pattern in the decadal ^7Be and ^{10}Be records during that period is eventually caused by SEP. This view is corroborated by Usoskin et al. (2009) who modelled the impact of solar energetic particles on the production and atmospheric concentration of ^7Be . They concluded that although extreme SEP events may dramatically enhance the ^7Be concentration in the upper polar stratosphere over several weeks, the near surface effect would be too small to be detected. Leaving the cause for the short-term mismatch between the decadal cycles of ^{10}Be and ^7Be actually unexplained, we finally address their pattern in relation to the GCR production signal.

Here, the question of a possible enhancement of the decadal, solar modulation at polar latitudes compared to the global mean is concerned. As intimately connected to the meridional stratospheric air mass transport (Bard et al., 1997), this issue remains conversely disputed. The phenomenon is of prime interest in the application of ^{10}Be in ice core studies (e.g. Bard et al., 1997;

Field et al., 2006; Heikkilä et al., 2009; Webber and Higbie, 2010) particularly in view of the reconstruction of a global production signal from high latitude ^{10}Be archives. As reflecting a more global signal (compared to ^7Be) through its higher stratospheric residence time, ^{10}Be may be less sensitive to production changes (which are especially large at high latitudes). Thus, depending on the meridional air mass exchange in the stratosphere the amplitude of the 11-yr solar cycle is expected to be generally smaller for ^{10}Be (compared to ^7Be). Given the 20% polar enhancement effect simulated by Field et al. (2006), the relatively large error range of our amplitude estimate exceeds this value by far. We could not quantify, therefore, a polar enhancement effect from the decadal ^7Be and ^{10}Be cycles seen in our NM data. Nevertheless, phase lag-correlation analyses of the neutron and our Be-isotope data indicated that ^{10}Be lags behind ^7Be by half a year, approximately, which suggests a more global relevance of the ^{10}Be record.

5. Conclusions and Outlook

Continuous 25 yr observations of the terrigenous ^{210}Pb and the cosmogenic ^{10}Be and ^7Be radionuclides from Neumayer Station provide the longest such records at coastal Antarctica. Moreover, they are the only ones with concurrent analyses of ionic aerosol species throughout Antarctica on that time scale. Detailed evaluation of these records in view of the radioisotope climatology revealed that a good deal of the monthly ^{210}Pb and ^7Be variability remains unexplained although the dominating sources of these species are relatively constant or, in case of ^7Be , vary regularly on the decadal scale. In all records, seasonal changes are characterized by maxima in the local summer half year. They appear to be the most obvious signal though being with 18–47% relatively weak compared to those of the source driven ion species. While the local effect of the surface inversion strength as well as large-scale transport effects may contribute to the ^{210}Pb seasonality (by essentially unknown fractions), subsidence of stratospheric air could be clearly attributed to the summer maxima shown by both Be-isotopes. The latter finding essentially manifests itself in the change of the $^{10}\text{Be}/^7\text{Be}$ ratio, which allows for the quantification of the stratospheric influence seen at (NM) surface level. Thus, this ratio helps greatly to assess the amount and timing of intrusion of other stratospheric species observed at NM like $^{14}\text{CO}_2$ (Levin et al., 2009).

Unexplained ‘meteorological noise’ dominates the inter-annual variability of all three species, which makes the identification of multi-annual cycles ambiguous. Nevertheless, a formally significant 4–6 yr mode appears to be inherent to the ^{210}Pb record, which resembles that of the southern annual mode (here ^{210}Pb lags the SAM index by about 18 month). No such mode is seen in the ^7Be time series (except a formally insignificant 2–3 yr oscillation) but, as expected, a clear decadal mode reflecting the solar cycle modulated isotope production.

Although the production signal is clearly visible in the ^7Be and ^{10}Be records there are still unexplained deviations between them, which challenge a useful quantification of the production-related decadal modes (which would, e.g. help deciding on the relevance of the ‘polar enhancement’ phenomenon). It is thus evident, that the inferring of the cosmogenic production time series (i.e. solar modulation parameter) remains difficult even based on atmospheric radionuclide records, which, unlike ice core data, are not subject to depositional noise. On the other hand, the characteristic relative amplitude of the decadal ^{10}Be signal (ranging between 10% and 35% in the atmosphere at NM) is quite comparable to what is observed in recent Antarctic firn core records, though the latter tend to show slightly higher decadal changes (Steig et al., 1998; Wegner, 2003). Also worth mentioning in view of related ice core studies is the 50% enhancement of the ^{10}Be summer maximum values over the annual mean in the atmospheric NM record. Although this summer excursion is much smaller compared to highly variable ionic aerosol species, it would make the generally less variable Antarctic ^{10}Be ice core signals sensitive to seasonal changes in the net snow accumulation rate. Interestingly, the only seasonally resolved ^{10}Be firn record from Antarctica derived by Pedro et al. (2010) in a coastal high accumulation area shows a quite similar seasonality as the atmospheric ^{10}Be record at NM. This concerns both, the relative amplitude and phase though the firn concentration is clearly dominated by wet aerosol deposition (representing only a minor time fraction relative to continuous atmospheric observations). Thus, the atmospheric long-term record of ^{10}Be (and also of ^{210}Pb) may be deployed in various ways to assess respective firn records in view of the air/firn transfer problem.

Efforts improving our understanding of the radionuclide variability at NM (and in the Antarctic troposphere) would primarily comprise: (i) dedicated modelling studies on the cosmogenic production variability influencing in the polar boundary layer concentration of Be-isotope as well as on the Stratosphere-Troposphere-Exchange, (ii) implementation of a continuous, atmospheric ^{10}Be record at NM in monthly resolution, (iii) detailed studies on the role of the surface inversion layer and associated meteorology coupled with daily radionuclide sampling and (iv) extension of these radionuclide observations to the Antarctic plateau replacing the (shutdown) measurements at South Pole. At least the two latter points are on their way through the ongoing establishment of a daily sampling programme at various coastal sites by the Comprehensive Nuclear Test Ban Treaty Organization (CTBTO) as well as by high volume aerosol sampling being now performed year round at the Dome Concordia inland station.

Acknowledgments

The authors would like to thank all the Neumayer overwintering crews: Without their careful field work, the 25 yr continu-

ous aerosol sampling would not have been possible. Similarly, we thank many students within the IUP ‘‘Glacier and Climate’’ working group for their steady efforts in obtaining the various radionuclide results. Special thanks go to Gert König-Langlo for advice on deploying the meteorological Neumayer observations and for providing us the data almost ready for use. We appreciate constructive criticism and the many suggestions of the two anonymous reviewers, which greatly helped improving the paper. The work was partly funded by the German Science Foundation, the EU-STEP programme and through special grants by the Alfred Wegener Institute for Polar and Marine Research to the Institut für Umweltphysik. The National Science Foundation under grant ANT-0739620 supported neutron monitors of the Bartol Research Institute.

References

- Aldahan, A., Hedfors, J., Possnert, G., Kulan, A., Berggren, A.-M., and co-authors. 2008. Atmospheric impact on beryllium isotopes as solar activity proxy. *Geophys. Res. Lett.* **35**, L21812, doi:10.1029/2008GL035189.
- Allen, R.M. and Smith, L.A. 1996. Monte Carlo SSA: detecting irregular oscillations in the presence of colored noise. *J. Clim.* **9**, 3373–3404.
- Auer M., Kutschera, W., Priller, A., Wagenbach, D., Wallner A., and co-authors. 2007. Measurement of ^{26}Al for atmospheric and climate research and the potential of $^{26}\text{Al}/^{10}\text{Be}$ ratio. *Nucl. Instr. Meth. B* **259**, 595–599.
- Bard, E., Raisbeck, G.M., Yiou, F., and Jouzel, J. 1997. Solar modulation of cosmogenic nuclide production over the last millennium: comparison between ^{14}C and ^{10}Be records. *Earth Planet. Sci. Lett.* **150**, 453–462.
- Barrie, L.A., et al. 2001. A comparison of large-scale atmospheric sulphate aerosol models (COSAM): overview and highlights. *Tellus* **53B**, 615–645.
- Bartol Research Institute, 2010. http://neutronm.bartol.udel.edu/~pyle/bri_table.html
- Beer, J., Siegenthaler, U., Bonani, G., Finkel, R.C., Oeschger, H., and co-authors. 1988. Information on past solar activity and geomagnetism from ^{10}Be in the Camp Century ice core. *Nature* **331**, 675–679.
- Broomhead, D.S., and King, G.P. 1986. Extracting qualitative dynamics from experimental data. *Phys. D* **20**, 217–236.
- Brost, R., Feichter, J., and Heimann, M. 1991. Three-dimensional simulation of ^7Be in a global climate model. *J. Geophys. Res.* **96**, 22423–22445.
- Considine, D.B., Bergmann, D.J., and Liu, H. 2005. Sensitivity of Global Modeling initiative chemistry and transport model simulations of radon-222 and lead-210 to input meteorological data. *Atmos. Chem. Phys.* **5**, 3389–3406.
- Dibb, J.E., Meeker, L.D., Finkel, R.C., Southon, J.R., Caffee, M.W., and co-authors. 1994. Estimation of stratospheric input into the Arctic troposphere: ^7Be and ^{10}Be in aerosols at Alert. *J. Geophys. Res.* **99**, 12855–12864.
- Dibb, J. E., Talbot, R.W., Lefer, B.L., Scheuer, E., Gregory, G.L., and co-authors. 1997. Distributions of beryllium-7 and lead-210 over the western Pacific: PEM West B, February – March, 1994. *J. Geophys. Res.* **102**, 28287–28302.

- Dibb, J. 2007. Vertical mixing above Summit, Greenland: insights into seasonal and high frequency variability from the radionuclide tracers ^7Be and ^{210}Pb . *Atmos. Environ.* **41**, 5020–5030.
- Dörr, H., and Münnich, K.O. 1990. ^{222}Rn flux and soil air concentration profiles in West-Germany. Soil ^{222}Rn as tracer for gas transport in the unsaturated soil zone. *Tellus* **42B**, 20–28.
- EML, 2010. US Environmental Measurements Laboratory SASP data base. <http://www.eml.st.dhs.gov/databases/>.
- Field, C., Schmidt, G.A., Koch, D., and Salyk, C. 2006. Modeling production and climate-related impacts on ^{10}Be concentration in ice cores. *J. Geophys. Res.* **111**, D15107, doi:10.1029/2005JD006410.
- Ghil, M., Allen, M.R., Dettinger, M.D., Ide, K., Kondashov, D., and co-authors. 2002. Advanced spectral methods for climatic time series. *Rev. Geophys.* **40**, 1–41.
- Gras, J.L. 1993. Condensation nucleus size distribution at Mawson, Antarctica: seasonal cycle. *Atmos. Environ.* **27A**(9), 1417–1425.
- Graustein, W.C., and Turekian, K.K. 1996. ^7Be and ^{210}Pb indicate an upper troposphere source for elevated ozone in the summertime subtropical free troposphere of the eastern North Atlantic. *Geophys. Res. Lett.* **23**, 539–542.
- Grinsted, A., Moore, J.C., and Jevrejeva, S. 2004. Application of the cross wavelet transform and wavelet coherence to geophysical time series. *Nonlinear Proc. Geophys.* **11**, 561–566.
- Hammer, S., Wagenbach, D., Preunkert, S., Pio, C., Schlosser, C., and co-authors. 2007. Lead-210 observations within CARBOSOL: a diagnostic tool for assessing the spatiotemporal variability of related chemical aerosol species? *J. Geophys. Res.* **112**, D23S03.
- Heikkilä, U., Beer, J., and Feichter, J. 2009. Meridional transport and deposition of atmospheric ^{10}Be . *Atmos. Chem. Phys.* **9**, 515–527.
- Heimann, M., Monfray, P., and Polian, G. 1990. Modeling the long-range transport of ^{222}Rn to subantarctic and antarctic areas. *Tellus* **42B**, 83–99.
- Hötzl, H., Rosner, G., and Winkler, R. 1991. Correlation of ^7Be concentrations in surface air and precipitation with the solar cycle. *Naturwissenschaften* **78**, 215–217.
- Holton, J.R., Haynes, P.H., McIntyre, M.E., Douglass, A.R., Hood, R.B., and co-authors. 1995. Stratosphere-troposphere exchange. *Rev. Geophys.* **33**, 403–439.
- Jacobs, G.A. and Mitchell, J.L. 1996. Ocean circulation variations associated with the Antarctic Circumpolar Wave. *Geophys. Res. Lett.* **23**(21), 2947–2950.
- James, P., Stohl, A., Forster, C., Eckhardt, S., Seibert, P., and co-authors. 2003. A 15-year climatology of stratosphere-troposphere exchange with a Lagrangian particle dispersion model: 2. Mean climate and seasonal variability. *J. Geophys. Res.* **108**(D12), 8522.
- Jordan, C.E., Dibb, J.E., and Finkel, R.C. 2003. $^{10}\text{Be}/^7\text{Be}$ tracer of atmospheric transport and stratosphere-troposphere exchange. *J. Geophys. Res.* **108**(D8), 4234.
- Koch, D.M., Jacob, D.J., and Graustein, W.C. 1996. Vertical transport of tropospheric aerosols as indicated by ^7Be and ^{210}Pb in a chemical tracer model. *J. Geophys. Res.* **101**(D13), 18651–18666.
- Koch, D.M., and Mann, M.E. 1996. Spatial and temporal variability of ^7Be surface concentrations. *Tellus* **48B**, 387–396.
- Kolb, W. 1992. Aktivitätskonzentrationen von Radionukliden in der bodennahen Luft Norddeutschlands und Nordnorwegens im Zeitraum von 1963 bis 1990. Report PTB-Ra-29, Physikalisch Technische Bundesanstalt, Braunschweig, Germany, 129.
- König-Langlo G., King, J.C. and Pettré, P. 1998. Climatology of the three coastal Antarctic stations Dumont d'Urville, Neumayer, and Halley. *J. Geophys. Res.*, **103**(D9), 10935–10946.
- Korschinek G., Bergmaier, A., Faestermann, T., Gerstmann, U.C., Knie, K., and co-authors. 2010. A new value for the half-life of ^{10}Be by Heavy-Ion Elastic Recoil Detection and liquid scintillation counting. *Nucl. Instr. Meth. Phys. Res. B*, **268**(2), 187–191.
- Kovaltsov, G.A. and Usoskin, I.G. 2010. A new 3D numerical model of cosmogenic nuclide ^{10}Be production in the atmosphere. *Earth Planet Science Lett.* **291**, 182–188.
- Kubik, P. and Christl, M. 2010. ^{10}Be and ^{26}Al measurements at the Zurich 6MV Tandem AMS facility. *Nucl. Instr. Meth. Phys. Res. B* **268**, 880–883.
- Lambert, G., Ardouin, B., and Sanak, J. 1990. Atmospheric transport of trace elements toward Antarctica. *Tellus*, **42B**, 76–82.
- Lee, H.N., Tositti, L., Zheng, H., and Bonasoni, P. 2007. Analyses and comparison of variations of ^7Be , ^{210}Pb , and $^7\text{Be}/^{210}\text{Pb}$ with ozone observations at two Global Atmospheric Watch stations from high mountains. *J. Geophys. Res.* **112**, D05303, doi:10.1029/2006JD007421.
- Legrand, M., and Wagenbach, D. 1999. Impact of the Cerro Hudson and Pinatubo volcanic eruptions on the Antarctic air and snow chemistry. *J. Geophys. Res.* **104**(D1), 1581–1596.
- Levin, I., Naegler, T., Kromer, B., Diehl, M., Francey, R.J., and co-authors. 2009. Observations and modeling of the global distribution and long-term trend of atmospheric $^{14}\text{CO}_2$. *Tellus* **62B**, 26–46.
- Masarik, J. and Beer, J. 1999. Simulation of particle fluxes and cosmogenic nuclide production in the earth's atmosphere. *J. Geophys. Res.* **D104**(10), 12099–13012.
- Masarik, J. and Beer, J. 2009. An updated simulation of particle fluxes and cosmogenic nuclide production in the Earth's atmosphere. *J. Geophys. Res.* **114**, D11103, doi:10.1029/2008JD010557.
- Minikin, A., Legrand, M., Hall, J., Wagenbach, D., Kleefeld, C., and co-authors. 1998. Sulfur-containing species (sulfate and MSA) in coastal Antarctic aerosol and precipitation. *J. Geophys. Res.* **103**, 10975–10990.
- Muscheler, R., Joos, F., Beer, J., Müller, S.A., Vonmoos, M., and co-authors. 2007. Solar activity during the last 1000yr inferred from radionuclide records. *Quarter. Sci. Rev.* **26**, 82–97.
- NOAA Earth System Research Laboratory 2010, <http://www.esrl.noaa.gov/psd/data/climateindices/>.
- O'Brian, K. 1979. Secular variations in the production of cosmogenic isotopes in the earth's atmosphere. *J. Geophys. Res.* **84**(A2), 423–431.
- Paatero, J., Hatakka, J., Holmén, K., Eneroth, K., and Viisanen Y., 2003. Lead-210 concentration in the air at Mt. Zeppelin, Ny-Ålesund, Svalbard. *Phys. Chem. Earth* **28**, 1175–1180.
- Pedro, J., v. Ommen, T., Curran, M., Morgan, V., and co-authors. 2006. Evidence for climate modulation of the ^{10}Be solar activity proxy. *J. Geophys. Res.* **111**, D21105.
- Pedro, J., Heikkilä, U., v. Ommen, T., and Smith, A.M. 2010. ^{10}Be in ice at high resolution: solar activity and climate signals observed and GCM-modeled in Law Dome ice cores. *Geophys. Res. Abstr.* **12**, EGU2010–11532.
- Piel, C., Weller, R., Huke, M. and Wagenbach, D. 2006. Atmospheric methane sulfonate and non-sea salt sulphate records at the EPICA deep-drilling site in Dronning Maud Land, Antarctica. *J. Geophys. Res.* **111**, D03304.
- Priller, A., Berger, M., Gäggeler, H.W., Gerasopoulos, E., Kubik, P.W., and co-authors. 2004. Accelerator mass spectrometry of particle-bound ^{10}Be . *Nuclear Instr. Meth. Phys. Res. B* **223–224**, 601–607.

- Raisbeck, G.M., Yiou, F., Fruneau, M., Loiseaux, L.M., Lieuvain, M., and co-authors. 1981. Cosmogenic ^{10}Be concentrations in Antarctic ice during the past 30000 years. *Nature* **292**, 825–826.
- Randel, W.J., and Wu, F. 2010. The polar summer tropopause inversion layer. *J. Atmos. Sci.* **67**, 2572–2581.
- Rehfeld, S. and Heimann, M. 1995. Three dimensional transport simulation of the radioactive tracers ^{210}Pb , ^7Be , ^{10}Be and ^{90}Sr . *J. Geophys. Res.* **100**(D12), 26.141–26.161.
- Roscoe, H.K. 2004. Possible descent across the Tropopause in Antarctic winter. *Adv. Space Res.* **33**(7), 1048–1052.
- Sanak, J., Gaudry, A., and Lambert, G. 1981. Size distribution of ^{210}Pb aerosols over oceans. *Geophys. Res. Lett.* **8**(10), 1067–1069.
- Sanak, J., Lambert, G., and Ardouin, B. 1985. Measurements of stratosphere-to-troposphere exchange in Antarctic by using short-lived cosmionuclides. *Tellus* **37B**, 109–115.
- Savoie, D.L., Prospero, J.M., Larsen, R.J., and Saltzman, E.S. 1992. Nitrogen and sulfur species in aerosols at Mawson, Antarctica, and their relationship to natural radionuclides. *J. Atmos. Chem.* **14**, 181–204.
- Steig, E.J., Morse, D.L., Waddington, E.D., and Polissar, P.J. 1998. Using the sunspot cycle to date ice cores. *Geophys. Res. Lett.* **25**(2), 163–166.
- Stohl, A., and Sodemann, H. 2010. Characteristics of atmospheric transport into the Antarctic troposphere. *J. Geophys. Res.* **115**, D02305.
- Stone, J., Fifield, K., Beer, J., Vonmoos, M., Obrist, C., and co-authors. 2004. Co-precipitated silver-metal oxide aggregates for accelerator mass spectrometry of ^{10}Be and ^{26}Al . *Nucl. Instr. Meth. Phys. Res. B* **223–224**, 272–277.
- Torrence, C. and Compo, G.P. 1998. A practical guide to wavelet analysis. *Bull. Am. Meteorol. Soc.* **79**, 61–78.
- Usoskin, I.G. and Kovaltsov, A. 2008. Production of cosmogenic ^7Be isotope in the atmosphere: full 3-D modeling. *J. Geophys. Res.* **113**, D12107.
- Usoskin, I.G., Field, C.V., Schmidt, G.A., Leppänen, A.P., Aldahan, A., and co-authors. 2009. Short-term production and synoptic influences on atmospheric ^7Be concentrations. *J. Geophys. Res.* **114**, D06108, doi:10.1029/2008JD011333.
- Vautard, R. and Ghil, M. 1989. Singular spectrum analysis in nonlinear dynamics with applications to paleoclimatic time series. *Physica D* **35**, 395–424.
- Wagenbach, D., Görlach, U., Moser U.K. and Münnich, K.O. 1988. Coastal Antarctic aerosol: the seasonal pattern of its chemical composition and radionuclide content. *Tellus* **40B**, 426–436.
- Wagenbach, D. 1996. Coastal Antarctica: atmospheric chemical composition and atmospheric transport. In: *Chemical Exchange Between the Atmosphere and Polar Snow* (ed. E.W. Wolff and R.C. Bales). NATO ASI Series, Vol. 43, Springer-Verlag, Berlin Heidelberg, 173–199.
- Wagenbach, D., Legrand, M., Fischer, H., Pichlmayer F. and Wolff, E.M. 1998. Atmospheric near surface nitrate at coastal Antarctic sites. *J. Geophys. Res.* **103**, 11007–11020.
- Wagner, G. 1998, *Die kosmogenen Radionuklide ^{10}Be und ^{36}Cl im Summit-GRIP-Eisbohrkern*, Dissertation, ETH Nr. 12864, Zurich, Switzerland.
- Webber, W.R., Higbie, P.R. and McCracken, K.G. 2007. Production of the cosmogenic isotopes ^3H , ^7Be , ^{10}Be , and ^{36}Cl in the Earth's atmosphere by solar and galactic cosmic rays. *J. Geophys. Res.* **112**, A10106.
- Webber, W.R. and Higbie, P.R. 2010. A comparison of new calculations of ^{10}Be production in the earth's polar atmosphere by cosmic rays with ^{10}Be concentration measurements in polar ice cores between 1939–2005—a troubling lack of concordance: paper #1. <http://arxiv.org/abs/1003.4989>.
- Wegner, A. 2003. *Die Geschichte der Sonnenaktivität im Antarktischen Eis Nachweis produktionsbedingter ^{10}Be -Schwankungen*, Diploma Thesis, Institut für Umweltphysik, University Heidelberg, Heidelberg, Germany.
- Weller, R., Jones, A.E., Wille, A., Jacobi, H.W., Sturges, H.P., and co-authors. 2002. Seasonality of reactive nitrogen oxides (NO_y) at Neumayer Station, Antarctica. *J. Geophys. Res.* **107**(D23), 4673.
- Weller, R., Levin, I., Wagenbach, D., and Minikin, A. 2006. The air chemistry observatory at Neumayer Stations (GvN and NM II) Antarctica. *Polarforschung* **76**(1–2), 39–46.
- Weller, R., Wöltjen, J., Piel, C., Resenberg, R., Wagenbach, D., and co-authors. 2008. Seasonal variability of crustal and marine trace elements in the aerosol at Neumayer Station, Antarctica. *Tellus* **60B**(5), 742–752.
- Weller, R., Wagenbach, D., Legrand, M., Elsässer, C., Tian-Kunze, X., and co-authors. 2011. Continuous 25-years aerosol records at coastal Antarctica: part 1. Inter-annual variability of ionic compounds and links to climate indices. *Tellus* **63B**, this issue.
- White, W.B. and Peterson, R.G. 1996. An Antarctic circumpolar wave in surface pressure, wind, temperature and sea-ice extent. *Nature* **380**, 699–702.
- Whittlestone, S. 1990. Radon daughter disequilibria in the lower marine boundary layer. *J. Atmos. Chem.* **11**, 27–42.

Supporting Information

Additional supporting information may be found in the online version of this article:

Appendix S1: Singular Spectrum Analysis.

Appendix S2: Auxiliary NM time series.

Appendix S3: Wavelet Analysis results.

Fig S1. Monthly (grey) and yearly (black) means of meteorological data at Neumayer Station together with the SAM and SOI circulation indices. While the SAM and SOI indices are monthly anomalies, the meteorological data sets are normalized by the respective mean values.

Fig. S2. Wavelet analysis of monthly means of ^7Be , ^{210}Pb together with SAM and SOI using a Morlet-6 wavelet and the code offered by Grinsted et al. (2004) (as based on Torrence and Compo (1998)). Thick black contour encloses area of 5% significance against red noise, in the light coloured area edge effects might distort the wavelet analysis. Colour code is associated with spectral power of the time series.

Fig. S3. Same as figure S2 but for meteorological parameters.

Please note: Wiley-Blackwell is not responsible for the content or functionality of any supporting materials supplied by the authors. Any queries (other than missing material) should be directed to the corresponding author for the article.